Evidence for $K_0^*(900)$ and Model-Independent Analysis Indications of the Scalar-Mesons Nature

Yu.S. Surovtsev (*BLTP, JINR, Dubna, Russia*),
T. Gutsche and V.E. Lyubovitskij (*Institut für Theoretische Physik, Universität Tübingen, Germany*)

Outline:

- **Motivation**
- **The coupled-channel formalism in model-independent approach**
- **Analysis of the isoscalar-scalar sector**
- **Analysis of the $K\pi$ scattering in the $I(J^P) = \frac{1}{2}(0^+)$ channel**
- **Discussion and conclusions**

Motivation

We present results of the coupled-channel analysis of data on processes $\pi\pi \to \pi\pi, K\overline{K}, \eta\eta, \eta\eta'$ in the the channel with $I^G J^{PC} = 0^+0^{++}$ and on the $K\pi$ scattering in the channel with $I(J^P) = \frac{1}{2}(0^+)$. Generally, scalar mesons are very intriguing objects constituting the Higgs sector of strong interactions and being the most direct bearers of information on the QCD vacuum structure.
An exceptional interest to this sector is supported by the fact that there, possibly indeed, we deal with a glueball $f_0(1500)$ (see, e.g., *C.Amsler, F.E.Close, PR D* ***53****, 295 (1996);* *C. Amsler* et al. *(PDG), PL B* ***667*** *(2008) 1.*).

However, as to parameters of the scalar mesons and even the status of some of them, there is a considerable disagreement (*C. Amsler* et al. *(PDG), PL B* ***667*** *(2008) 1.*).

Especially this concerns the $f_0(600)/\sigma$-meson and $K_0^*(900)/\kappa(800)$. In view of these circumstances, there are the known problems as to determining a QCD nature of the observed mesonic states and their assignment to the quark-model configurations in spite of a big amount of work devoted these problems (see, e.g., *V.V.Anisovich, IJMP A **21, 3615 (2006)* and references therein).**

Here we have applied to analyses of experimental data a model-independent method based only on the first principles (analyticity and unitarity) (*D.Krupa, V.Meshcheryakov, Yu.Surovtsev, NC A **109, 281 (1996) – KMS, 96*). That approach permits us to omit theoretical prejudice in extracting the resonance parameters. Considering the obtained disposition of resonance poles on the Riemann surface, obtained coupling constants with channels and resonance masses, we draw definite conclusions about nature of the investigated states.**

The coupled-channel formalism in model-independent approach

Our model-independent method which essentially utilizes an uniformizing variable can be used only for the 2-channel case and under some conditions for the 3-channel one. Only in these cases we obtain a simple symmetric (easily interpreted) picture of the resonance poles and zeros of the S-matrix on the uniformization plane.

The S-matrix is determined on the 4- and 8-sheeted Riemann surfaces for the 2- and 3-channel cases, respectively. The matrix elements $S_{\alpha\beta}$, where $\alpha, \beta = 1, 2, 3$ denote channels, have the right-hand cuts along the real axis of the s complex plane (s is the invariant total energy squared), starting with the channel thresholds s_i $(i = 1, 2, 3)$, and the left-hand cuts.

The Riemann-surface sheets are numbered according to the signs of analytic continuations of the channel momenta $k_i = \sqrt{s - s_i}/2 \quad (i = 1, 2, 3)$ as follows:

	I	II	III	IV	V	VI	VII	VIII
$\mathrm{Im}k_1$	+	−	−	+	+	−	−	+
$\mathrm{Im}k_2$	+	+	−	−	−	−	+	+
$\mathrm{Im}k_3$	+	+	+	+	−	−	−	−

The resonance representations on the Riemann surfaces are obtained with the help of formulas from (*KMS, 96*), expressing analytic continuations of the S-matrix elements to unphysical sheets in terms of those on sheet I that have only the resonances zeros (beyond the real axis), at least, around the physical region.

In the 2-channel case, we obtain 3 types of resonances described by a pair of conjugate zeros on sheet I only in S_{11} – the type (a), only in S_{22} – (b), and in each of S_{11} and S_{22} – (c).

In the 3-channel case, we obtain 7 types of resonances corresponding to 7 possible situations when there are resonance zeros on sheet I only in S_{11} – (a); S_{22} – (b); S_{33} – (c); S_{11} and S_{22} – (d); S_{22} and S_{33} – (e); S_{11} and S_{33} – (f); S_{11}, S_{22}, and S_{33} – (g).
The resonance of every type is represented by the pair of complex-conjugate clusters (of poles and zeros on the Riemann surface). The cluster kind is related to the nature of state. For example, if we consider the $\pi\pi$, $K\overline{K}$ and $\eta\eta$ channels, then a resonance, coupled relatively more strongly to the $\pi\pi$ channel than to the $K\overline{K}$ and $\eta\eta$ ones is described by the cluster of type (a). In the opposite case, it is represented by the cluster of type (e) (say, the state with the dominant $s\bar{s}$ component). The flavour singlet (*e.g.*, glueball) must be represented by the cluster of type (g) (of type (c) in the 2-channel consideration) as a necessary condition for the ideal case, if this state lies above the thresholds of considered channels.

Note that whereas cases (a), (b) and (c) can be simply related to the representation of resonances by Breit-Wigner forms, cases (d), (e), (f) and (g) practically are lost at the Breit-Wigner description.

We can distinguish, in a model-independent way, a bound state of colourless particles (*e.g.*, $K\overline{K}$ molecule) and a $q\bar{q}$ bound state. Just as in the 1-channel case, the existence of the particle bound-state means the presence of a pole on the real axis under the threshold on the physical sheet, so in the 2-channel case, the existence of the bound-state in channel 2 ($K\overline{K}$ molecule) that, however, can decay into channel 1 ($\pi\pi$ decay), would imply the presence of the pair of complex conjugate poles on sheet II under the second-channel threshold without the corresponding shifted pair of poles on sheet III.

In the 3-channel case, the bound-state in channel 3 ($\eta\eta$) that, however, can decay into channels 1 ($\pi\pi$ decay) and 2 ($K\overline{K}$ decay), is represented by the pair of complex conjugate poles on sheet II and by the pair of shifted poles on sheet III under the $\eta\eta$ threshold without the corresponding poles on sheets VI and VII. This test (*D. Morgan, M.R. Pennington, PR D* ***48****, 1185 (1993); KMS, 96*) **is the multichannel analogue of the known Castillejo–Dalitz–Dyson poles in the one-channel case. According to this test, earlier in** (*KMS, 96*), **we rejected interpretation of the $f_0(980)$ as the $K\overline{K}$ molecule because this state is represented by the cluster of type (a) in the 2-channel analysis of processes $\pi\pi \to \pi\pi, K\overline{K}$ and, therefore, does not satisfy the necessary condition to be the $K\overline{K}$ molecule.**

We use the Le Couteur-Newton relations (*K.J.LeCouteur, Proc.Roy.Soc. A **256, 115 (1960); R.G.Newton, J.Math.Phys. **2**, 188 (1961); M.Kato, Ann.Phys. **31**, 130 (1965)*). They express the S-matrix elements of all coupled processes in terms of the Jost matrix determinant $d(k_1, \cdots, k_n)$ that is a real analytic function with the only square-root branch-points at $k_i = 0$.**

The important branch points, corresponding to the thresholds of the coupled channels and to the crossing ones, are taken into account in the proper uniformizing variable.

On the uniformization plane, the pole-cluster representation of the resonance is the good one.

Analysis of the isoscalar-scalar sector

Considering the S-waves of processes

$$\pi\pi \to \pi\pi, K\overline{K}, \eta\eta, \eta\eta'$$

in the model-independent approach, we have performed 2 variants of the 3-channel analysis.
Variant I: The combined analysis of $\pi\pi \to \pi\pi, K\overline{K}, \eta\eta$.
Variant II: Analysis of $\pi\pi \to \pi\pi, K\overline{K}, \eta\eta'$.
Influence of the $\eta\eta'$-channel in the I case and of the $\eta\eta$ in the II one are taken into account in the background.

In the new uniformizing variable used, we neglect the $\pi\pi$-threshold branch point (however, unitarity on the $\pi\pi$-cut is considered) and take into account the threshold branch-points related to two remaining channels and the left-hand branch-point at $s = 0$ concerned the crossed channels.

It is

$$w = 2\frac{m_\eta k_2 + m_K k_3}{\sqrt{s(m_\eta^2 - m_K^2)}} \qquad \text{for variant I,}$$

and

$$w' = \frac{(m_\eta + m_{\eta'})k_2' + 2m_K k_3'}{\sqrt{s[\frac{1}{4}(m_\eta + m_{\eta'})^2 - m_K^2]}} \qquad \text{for variant II.}$$

All, related to variant II, are primed.

On the w-plane, the Le Couteur-Newton relations are

$$S_{11} = \frac{d^*(-w^*)}{d(w)}, \qquad S_{22} = \frac{d(-w^{-1})}{d(w)}, \qquad S_{33} = \frac{d(w^{-1})}{d(w)},$$

$$S_{11}S_{22} - S_{12}^2 = \frac{d^*(w^{*-1})}{d(w)}, \qquad S_{11}S_{33} - S_{13}^2 = \frac{d^*(-w^{*-1})}{d(w)}.$$

$$d = d_B d_{res}, \qquad d_{res}(w) = w^{-\frac{M}{2}} \prod_{r=1}^{M} (w + w_r^*)$$

M is the number of resonance zeros.

$$d_B = \exp[-i(a + \sum_{n=1}^{3} \frac{k_n}{m_n}(\alpha_n + i\beta_n))],$$

$$\alpha_n = a_{n1} + a_{n\sigma}\frac{s - s_\sigma}{s_\sigma}\theta(s - s_\sigma) + a_{nv}\frac{s - s_v}{s_v}\theta(s - s_v),$$

$$\beta_n = b_{n1} + b_{n\sigma}\frac{s - s_\sigma}{s_\sigma}\theta(s - s_\sigma) + b_{nv}\frac{s - s_v}{s_v}\theta(s - s_v).$$

s_σ – the $\sigma\sigma$ threshold; s_v – the combined threshold of many opening channels in the range of ~ 1.5 GeV ($\eta\eta'$, $\rho\rho$, $\omega\omega$).

In variant II (the uniformizing variable w'),

$$a'_{n\eta}\frac{s - 4m_\eta^2}{4m_\eta^2}\theta(s - 4m_\eta^2) \quad \text{and} \quad b'_{n\eta}\frac{s - 4m_\eta^2}{4m_\eta^2}\theta(s - 4m_\eta^2)$$

should be added to α'_n and β'_n, respectively.

For the $\pi\pi$ scattering, the data from the threshold to 1.89 GeV are taken from (*B.Hyams* et al., *NP B* ***64****, 134 (1973); ibid.* ***100****, 205 (1975); A.Zylbersztejn* et al., *PL B* ***38****, 457 (1972); P.Sonderegger, P.Bonamy, in Proc. 5th Intern. Conf. on Elem. Part., Lund, 1969, paper 372; J.R.Bensinger* et al., *PL B* ***36****, 134 (1971); J.P.Baton* et al., *PL B* ***33****, 525, 528 (1970); P.Baillon* et al., *PL B* ***38****, 555 (1972); L.Rosselet* et al., *PR D* ***15****, 574 (1977); A.A.Kartamyshev* et al., *Pis'ma v ZhETF* ***25****, 68 (1977); A.A. Bel'kov* et al., *Pis'ma v ZhETF* ***29****, 652 (1979)*). For $\pi\pi \to K\overline{K}$, practically all the accessible data are used (***W.Wetzel*** et al., *NP B* ***115****, 208 (1976); V.A.Polychronakos* et al., *PR D* ***19****, 1317 (1979); P.Estabrooks, PR D* ***19****, 2678 (1979); D.Cohen* et al., *PR D* ***22****, 2595 (1980); G.Costa* et al., *NP B* ***175****, 402 (1980); A.Etkin* et al., *PR D* ***25****, 1786 (1982)*). For $\pi\pi \to \eta\eta$, we used data for $|S_{13}|^2$ from the threshold to 1.72 GeV (*F.Binon* et al., *NC A* ***78****, 313 (1983)*). For $\pi\pi \to \eta\eta'$, the data for $|S_{13}|^2$ from the threshold to 1.813 GeV are taken from (*F. Binon* et al., *NC A* ***80****, 363 (1984)*).**

We considered the case with all five resonances discussed below 1.9 GeV. In variant I, the $f_0(600)$ is described by the cluster of type (a); $f_0(1370)$, type (c); $f_0(1500)$, type (g); $f_0(1710)$, type (b); the $f_0(980)$ is represented only by the pole on sheet II and shifted pole on sheet III in both variants.

Satisfactory description: for the $\pi\pi$-scattering from about 0.4 to 1.89 GeV ($\chi^2/\mathrm{NDF} = 155.319/(165-34) \approx 1.19$); for $\pi\pi \to K\overline{K}$, from the threshold to about 1.6 GeV ($\chi^2/\mathrm{NDF} = 147.169/(120-33) \approx 1.69$); for $\pi\pi \to \eta\eta$, from the threshold to 1.72 GeV ($\chi^2/\mathrm{N.exp.points} \approx 0.86$).

The total χ^2/NDF is $314.452/(301-41) \approx 1.21$.

The background parameters are: $a = 0.1199$, $a_{11} = 0.2813$, $a_{1\sigma} = -0.008$, $a_{1v} = 0$, $b_{11} = 0$, $b_{1\sigma} = 0$, $b_{1v} = 0.0462$, $a_{21} = -1.3267$, $a_{2\sigma} = -0.5829$, $a_{2v} = -7.544$, $b_{21} = 0.0344$, $b_{2\sigma} = 0$, $b_{2v} = 6.862$, $b_{31} = 0.6386$, $b_{3\sigma} = 0.4384$, $b_{2v} = 0$; $s_\sigma = 1.638\ \mathrm{GeV}^2$, $s_v = 2.085\ \mathrm{GeV}^2$.

The combined description of processes $\pi\pi \to \pi\pi, K\overline{K}, \eta\eta'$ (variant II) is even better due to the more detailed representation of the background:
the $f_0(600)$ is described by the cluster of type (a$'$);
$f_0(1370)$, type (b$'$); $f_0(1500)$, type (d$'$); $f_0(1710)$, type (c$'$).
For the
$\pi\pi$-scattering, $\chi^2/\mathrm{NDF} = 129.854/(165-31) \approx 0.97$.
for $\pi\pi \to K\overline{K}$, $\chi^2/\mathrm{NDF} = 150.904/(120-31) \approx 1.68$;
for $\pi\pi \to \eta\eta'$, $\chi^2/\mathrm{N.exp.points} \approx 0.3$.
The total χ^2/NDF for these three processes is
$283.151/(293-38) \approx 1.11$!
The background parameters are:
$a' = 0.2315$, $a'_{11} = 0$, $a'_{1\eta} = -0.0616$, $a'_{1\sigma} = 0.0298$,
$a'_{1v} = 0.0622$, $b'_{11} = b'_{1\eta} = b'_{1\sigma} = 0$, $b'_{1v} = 0.0449$,
$a'_{21} = -3.1359$, $a'_{2\eta} = 0$, $a'_{2\sigma} = 0.4866$, $a'_{2v} = -4.532$,
$b'_{21} = 0$, $b'_{2\eta} = -0.7478$, $b'_{2\sigma} = 2.5545$, $b'_{2v} = 1.948$,
$b'_{31} = 0.4489$, $s_\sigma = 1.638\ \mathrm{GeV}^2$, $s_v = 2.126\ \mathrm{GeV}^2$.

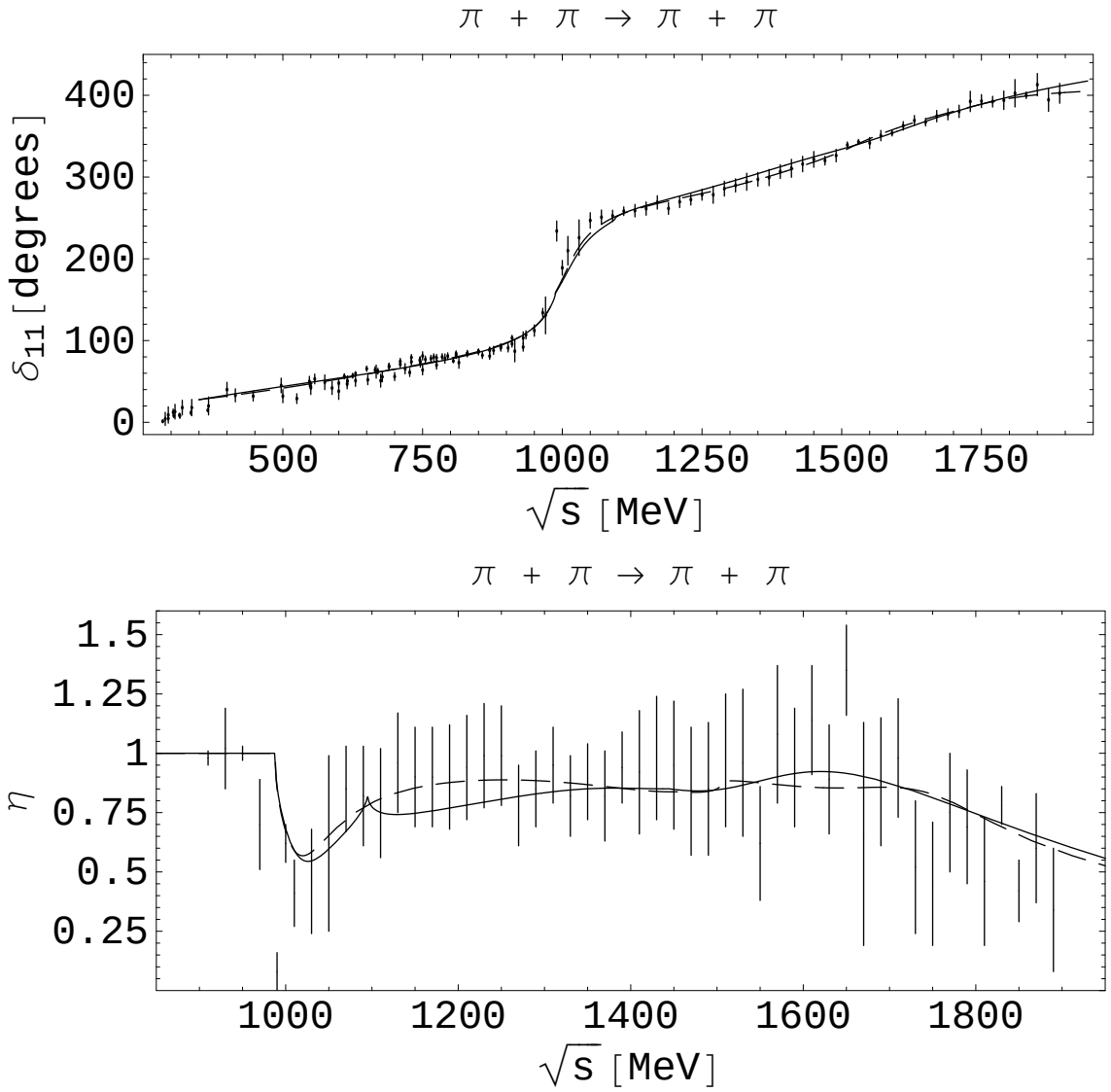

Figure 1: The phase shift and module of the $\pi\pi$-scattering S-wave matrix element. The solid curve – variant I; the dashed curve – variant II.

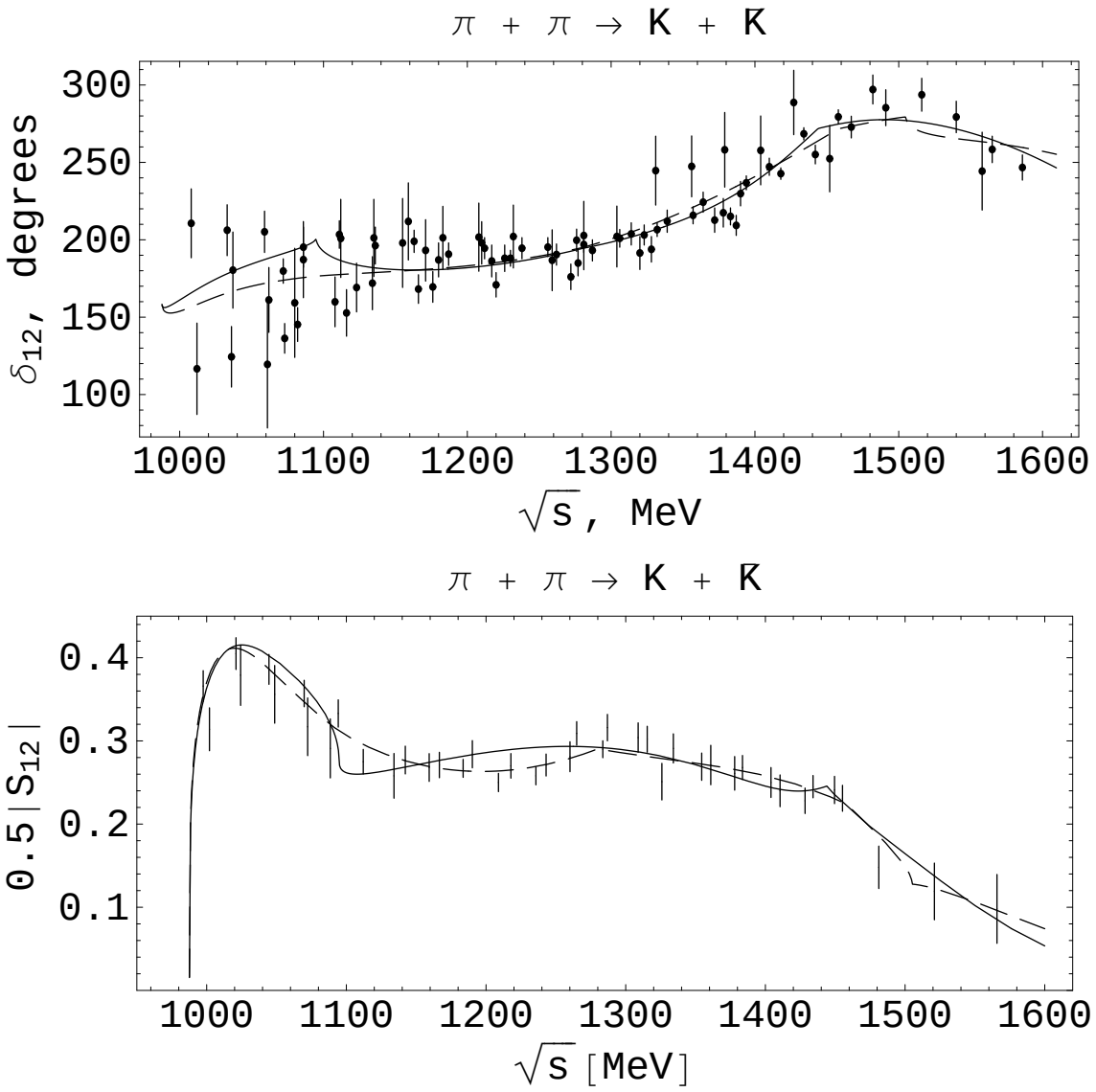

Figure 2: The phase shift and module of the $\pi\pi \to K\overline{K}$ S-wave matrix element. The solid curve – variant I; the dashed curve – variant II.

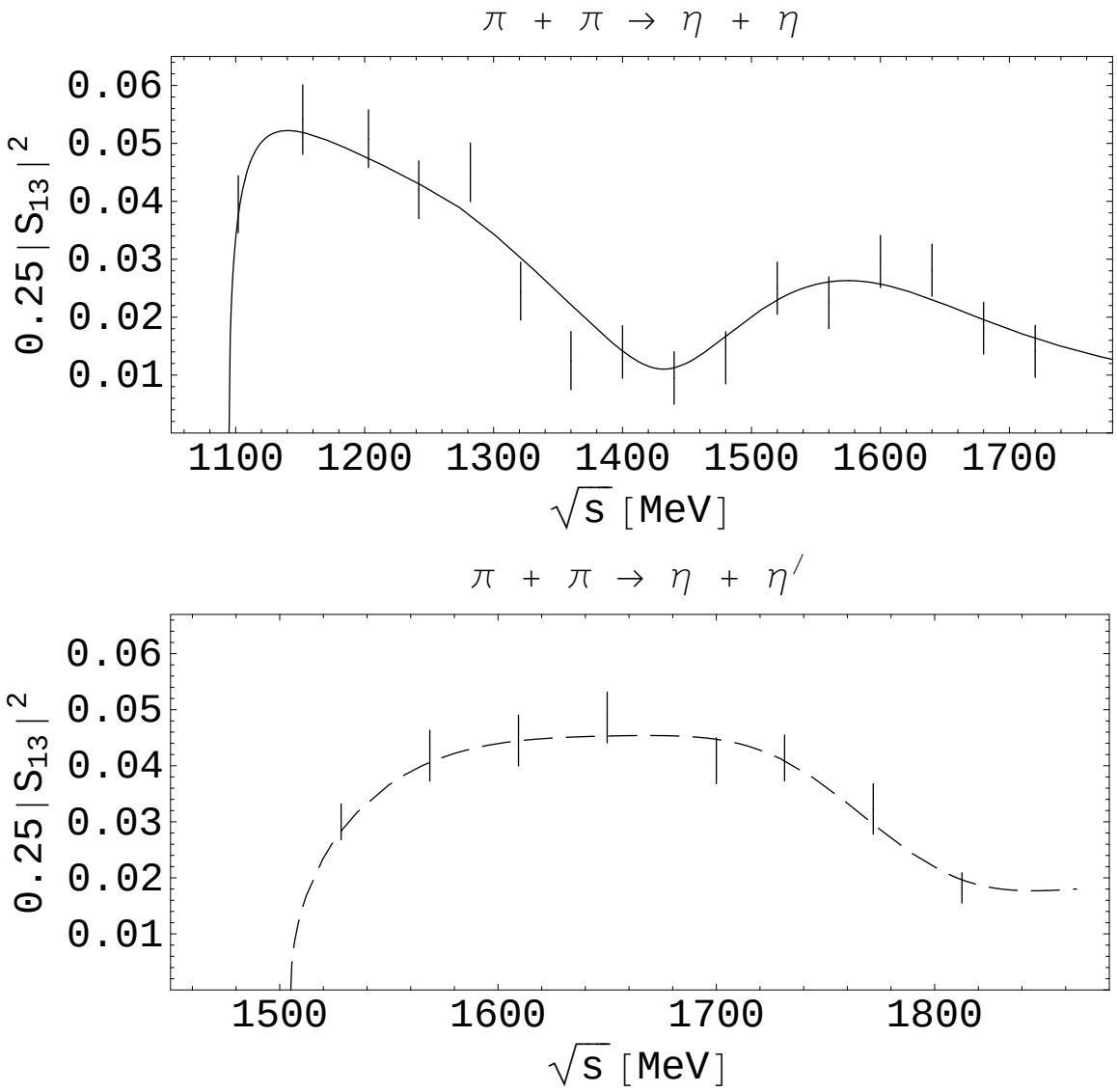

Figure 3: The squared modules of the $\pi\pi \to \eta\eta$ (upper figure) and $\pi\pi \to \eta\eta'$ (lower figure) S-wave matrix elements.

Let us indicate the obtained pole clusters for resonances on the complex energy plane $\sqrt{s}$. In variant I, poles on sheets IV, VI, VIII and V, corresponding to the $f_0(1500)$, are of the 2nd and 3rd order, respectively (this is an approximation). In variant II, poles on sheets IV and V, corresponding to the $f_0(1500)$, are of the 2nd order. $\sqrt{s_r} = \mathrm{E}_r - i\Gamma_r$.

Table 1: Pole clusters for the f_0-resonances in variant I.

Sheet		II	III	IV	V	VI	VII	VIII
$f_0(600)$	E_r	550.05±13	624±14			628.9±16	555.4±15	
	Γ_r	559±17	559±19			559±18	559±20	
$f_0(980)$	E_r	1011.9±4	978.2±9					
	Γ_r	36.4±6	56.3±10					
$f_0(1370)$	E_r				1396.1±16	1396.1±18	1396.1±18	1396.1±13
	Γ_r				287.1±17	270.5±15	155.7±9	172.3±7
$f_0(1500)$	E_r	1501.2±11	1495.8±13	1501.2±12	1497.7±12.5	1510.4±16	1502±12	1501.2±10
	Γ_r	357.4±15	140.7±12	238±13	140.5±14	186.9±17	90.9±11	356.4±14
$f_0(1710)$	E_r		1718±12	1718±10	1718±13	1718±15		
	Γ_r		149.5±9	166.3±8	321.9±14	305.1±13		

Table 2: Pole clusters for the f_0-resonances in variant II.

Sheet		II	III	IV	V	VI	VII	VIII
$f_0(600)$	E_r	558.7±8	564.3±10			541.3±12	535.7±12.5	
	Γ_r	529±11	529±12			529±14	529±13	
$f_0(980)$	E_r	1009±3	986±6					
	Γ_r	31.8±4	57.4±5.5					
$f_0(1370)$	E_r		1411.6±9	1411.6±11	1428.4±13	1428.4±14		
	Γ_r		215.6±10	235±12	235±12	215.6±19		
$f_0(1500)$	E_r	1496.9±12	1503±10	1496.9±13	1496.9±14	1494.6±12	1496.9±15	
	Γ_r	198.5±15	236±10	193.1±9	198.5±11	193.7±8.5	193.1±10	
$f_0(1710)$	E_r				1743±12	1743±13	1743±12	1743±10
	Γ_r				144.1±9	111.5±8	82.1±8	114.7±7

Note a surprising result obtained for the $f_0(980)$. It turns out that this state lies slightly above the $K\overline{K}$ threshold and is described by the pole on sheet II and by the shifted pole on sheet III under the $\eta\eta$ threshold without the corresponding poles on sheets VI and VII, as it was expected for standard clusters. This corresponds to the description of the $\eta\eta$ bound state.

For subsequent conclusions, let us mention the results for coupling constants from our previous 2-channel analysis of processes $\pi\pi \to \pi\pi, K\overline{K}$ (*Yu.S.Surovtsev, D.Krupa, M.Nagy, EPJ A* ***15**, 409 (2002)*): g_1 is the coupling constant with $\pi\pi$; g_2, with $K\overline{K}$.**

	$f_0(600)$	$f_0(980)$	$f_0(1370)$	$f_0(1500)$
g_1, GeV	0.652 ± 0.065	0.167 ± 0.05	0.116 ± 0.03	0.657 ± 0.113
g_2, GeV	0.724 ± 0.1	0.445 ± 0.031	0.99 ± 0.05	0.666 ± 0.15

The $f_0(980)$ and the $f_0(1370)$ are coupled essentially more strongly to the $K\overline{K}$ system than to the $\pi\pi$ one, *i.e.*, they have a dominant $s\bar{s}$ component. The $f_0(1500)$ has the approximately equal coupling constants with the $\pi\pi$ and $K\overline{K}$, which apparently could point to its dominant glueball component. In the 2-channel case, $f_0(1710)$ is represented by the cluster corresponding to a state with the dominant $s\bar{s}$ component.

Our 3-channel conclusions on the basis of resonance cluster types generally confirm the ones drawn in the 2-channel analysis (besides the above surprising conclusion about the $f_0(980)$ nature).
Masses and widths of states should be calculated from the pole positions.

$$T^{res} = \sqrt{s}\Gamma_{el}/(m_{res}^2 - s - i\sqrt{s}\Gamma_{tot})$$

Table 3: Masses and total widths of the f_0-resonances (in MeV).

	Variant I		Variant II	
State	m_{res}	Γ_{tot}	m_{res}	Γ_{tot}
$f_0(600)$	784.6	1118	769.4	1058
$f_0(980)$	1012.6	72.8	1009.5	63.6
$f_0(1370)$	1406.7	344.6	1431	470
$f_0(1500)$	1542.9	712.8	1510	397
$f_0(1710)$	1724.5	299	1746.8	229.4

Analysis of the $K\pi$ scattering in the $I(J^P) = \frac{1}{2}(0^+)$ channel

When analyzing data (*D. Aston et al., NP B* ***296****, 493 (1988)*) for the module of the $K^-\pi^+$-scattering amplitude $T = (S-1)/2i$ and its phase shift δ in the $I(J^P) = \frac{1}{2}(0^+)$ channel, we applied the model-independent method taking into account in the uniformizing variable the branch-points related to the thresholds of the $K\pi$ and $K\eta$ channels assuming that the influence of remaining channels and the left-hand cuts can be accounted via the background. The corresponding uniformizing variable has the form:

$$v = \frac{\sqrt{s - s_0} + \sqrt{s - s_1}}{\sqrt{s_1 - s_0}}$$

where s_0 and s_1 are the thresholds of the $K^-\pi^+$ and $K^0\eta$ channels, respectively.

The 2-channel S-matrix element of $K\pi$-scattering is taken in the form

$$S = S_{res} e^{2i\delta_{bg}}$$

where the resonance part

$$S_{res} = \frac{d(-v^{-1})}{d(v)}$$

has no cuts on the v-plane. The $d(v)$-function is

$$d(v) = v^{-M} \prod_{n=1}^{M} (1 - v_n^* v)(1 + v_n v),$$

where M is the number of pairs of the conjugate zeros corresponding to resonances.

The phase

$$\delta_{bg} = \sqrt{\frac{s - s_0}{s}}(a + ib)$$

describes the background: a relates to its elastic part, b to the inelastic one.

Since the question stands about the status of the $K_0^*(900)$, first we carried out the analysis considering only one resonance $K_0^*(1450)$ of type (a). It is possible to obtain a satisfactory description with the total $\chi^2/\mathrm{NDF} = 125.85/(74-6) \approx 1.85$. Omitting three experimental points at 826.67, 1560.01 and 1591.12 MeV for the module of amplitude and the points at 867.86, 1016 and 1384.11 MeV for the phase shift δ which give the anomalously-large contribution to the χ^2, we obtained the total $\chi^2/\mathrm{NDF} = 92.09/(68-6) \approx 1.48$.

The calculated mass and total width were 1428 and 282 MeV, respectively, and the background parameters $a = 0.6951$ and $b = -0.0614$. A negative sign of the quantity b means the increasing inelastic part of the background.

It is important: *The increasing inelastic background part implies a necessity to consider explicitly some physical phenomenon*.

In the previous analysis of scalar sector, the analogous situation in variant II implied necessity of the explicit consideration of the $\eta\eta$-threshold branch-point.

In the given case, the increasing inelastic background part implies necessity to consider explicitly one more resonance of the expected type (b). Indeed, it turned out that for the reasonable description two resonances, $K_0^*(900)$ of type (b) and $K_0^*(1450)$ of type (a), should be considered. The total χ^2/NDF is $128.296/(74-9) \approx 1.97$. Omitting three points at 826.67, 1560.01 and 1591.12 MeV for the module of amplitude and the points at 827.45, 1384.11 and 1505.32 MeV for the phase shift which give the anomalously-large contribution to the χ^2, we obtain the total $\chi^2/\mathrm{NDF} = 75.707/(68-9) \approx 1.28$, *i.e.*, the description is better, and, furthermore and this is principal, *the background parameter* $\boldsymbol{b}$ *equals zero in this case*.

In Table, the pole-clusters of the obtained resonances are shown on the lower $\sqrt{s}$-half-plane (in MeV) of the 4-sheeted Riemann surface (the poles on the upper half-plane are not shown).

	II	III	IV
$K_0^*(900)$		$859.9 - i221.6$	$885.6 - i280.8$
$K_0^*(1450)$	$1441.7 - i172.3$	$1430 - i144$	

These pole-clusters mean that the $K_0^*(1450)$ is coupled mainly with the $K\pi$ channel, whereas the $K_0^*(900)$ is coupled weaker with this channel than with other ones such as the $K\eta$ and $K\eta'$ channels.

Masses and total widths can be calculated from the pole positions on sheet II for resonance of type (a) and on sheet IV for resonance of type (b).

$$T^{res} = \frac{\sqrt{s}\ \Gamma_{el}}{m_{res}^2 - s - i\sqrt{s}\ \Gamma_{tot}},$$

	m_{res} [MeV]	Γ_{tot} [MeV]
$K_0^*(900)$	929	561.6
$K_0^*(1450)$	1452	344.6

The background phase shift

$$\delta_{bg} = \sqrt{(s - s_0)/s}\ a$$

turned out to be elastic with the only parameter $a = 0.6503$. This means that the influence of other channels such as $K\pi\pi\pi$ and $K\pi\sigma$ is negligible, except for the $K^0\eta'$ channel, at opening of which there is a small deviation of our curve for the module of amplitude from the data.

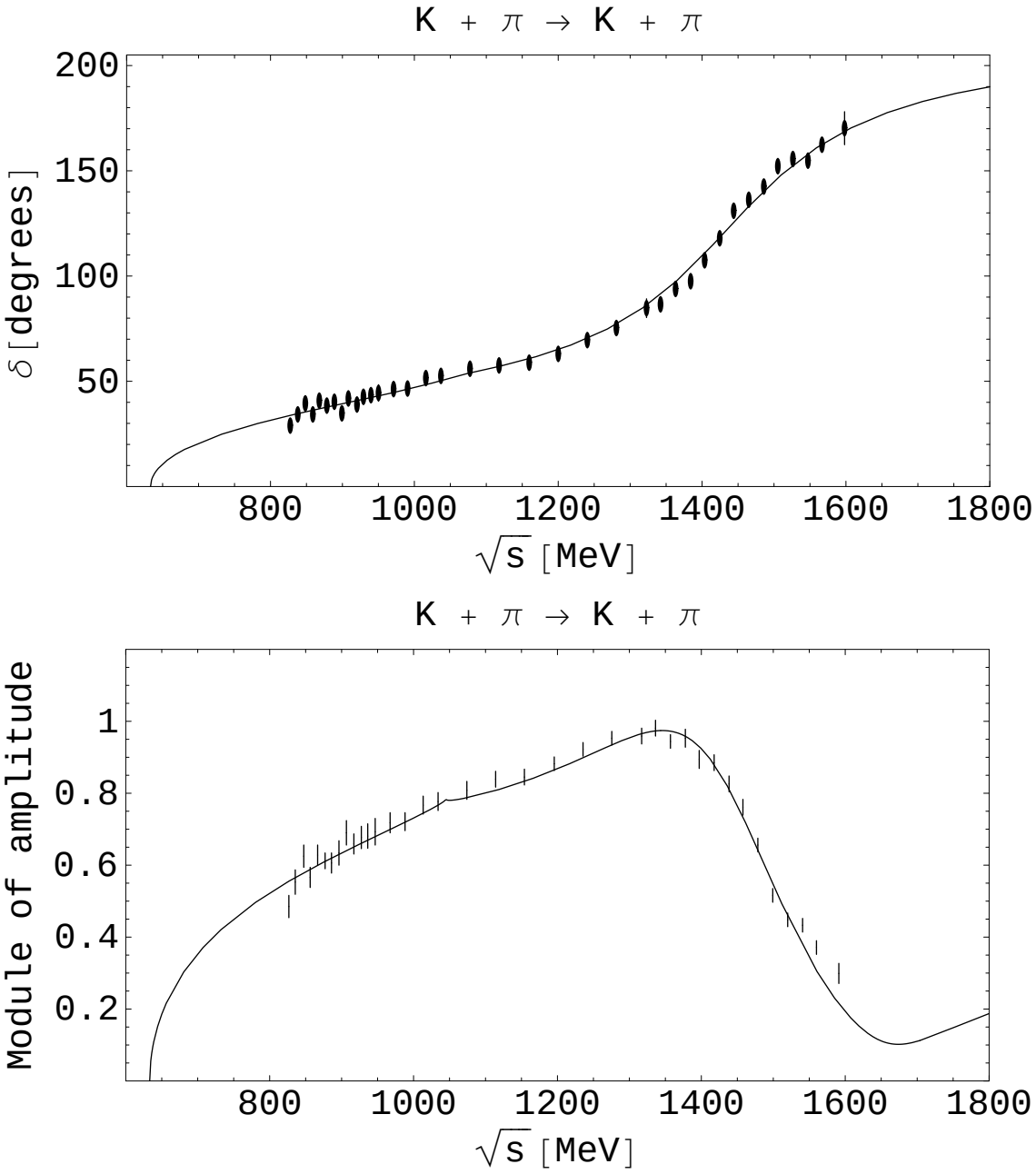

Figure 4: The phase shift and module of amplitude of the $K\pi$ scattering in the $I(J^P) = \frac{1}{2}(0^+)$ channel.

Discussion and conclusions

- **In the combined model-independent analysis of data on the $\pi\pi \to \pi\pi, K\overline{K}, \eta\eta, \eta\eta'$ processes in the $I^G J^{PC} = 0^+0^{++}$ channel, an additional confirmation of the σ-meson with mass 785 MeV is obtained. This value remarkably accords with prediction ($m_\sigma \approx m_\rho$) on the basis of mended symmetry by S. Weinberg (*PRL* ***65****, 1177 (1990)*).**
- **Indication for $f_0(980)$ to be the $\eta\eta$ bound state is obtained. From the point of view of quark structure, this is the 4-quark state. Maybe, this is consistent somehow with arguments in favour of the 4-quark nature of $f_0(980)$ (*N.N.Achasov, NP A* ***675****, 279c (2000); M.N.Achasov* et al.*, PL B* **438**, *441 (1998); ibid.* **440**, *442 (1998)*).**

- **The $f_0(1370)$ and $f_0(1710)$ have the dominant $s\bar{s}$ component. Conclusion about the $f_0(1370)$ quite well agrees with the one of work of Crystal Barrel Collaboration (*C.Amsler* et al., *PL B* ***355***, *425 (1995)*) where the $f_0(1370)$ is identified as $\eta\eta$ resonance in the $\pi^0\eta\eta$ final state of the $\bar{p}p$ annihilation at rest. Conclusion about the $f_0(1710)$ is quite consistent with the experimental facts that this state is observed in $\gamma\gamma \to K_S K_S$ (*S.Braccini, Proc. Workshop on Hadron Spectroscopy, Frascati Phys. Series* ***XV***, *53 (1999)*) and not observed in $\gamma\gamma \to \pi^+\pi^-$ (*R.Barate* et al., *PL B* ***472***, *189 (2000)*).**

- **As to the $f_0(1500)$, we suppose that it is practically the eighth component of octet mixed with a glueball being dominant in this state. Its biggest width among enclosing states tells also in behalf of its glueball nature (*V.V.Anisovich et al., NP Proc.Suppl. A****56****, 270 (1997)*).**

- **In the model-independent analysis of the $K\pi$ scattering data (*D. Aston et al., NP B* ***296****, 493 (1988)*) in the $I(J^P) = \frac{1}{2}(0^+)$ channel, an evidence for existence of the $K_0^*(900)$ with the mass 929 MeV and total width 564 MeV is obtained. This state should be coupled weaker with the $K\pi$ channel than with the $K\eta$ and/or $K\eta'$ ones. Our mass value differs from the average one (672±40 MeV) cited in the PDG tables of 2008, whereas the width practically coincides. Our values of the mass and width correspond most near to the ones (909^{+65}_{-30} and 545^{+235}_{-110} MeV, respectivly) from work (*S.Ishida* et al., *PTP* ***98****, 621 (1997)*), obtained in the analysis of the $K\pi$ scattering using an interfering Breit-Wigner amplitudes. However, unlike the indicated work, *we did not need the repulsive background*, not very clear in the $K\pi$ scattering.**

- **The second K_0^* resonance in the $K\pi$ scattering has the mass 1452 MeV and total width 346 MeV in some accordance with the values cited in the PDG tables.**
- **We propose a following assignment of scalar mesons below 1.9 GeV to lower nonets, when excluding the $f_0(980)$ as the $\eta\eta$ bound state. The lowest nonet: the isovector $a_0(980)$, the isodoublet $K_0^*(900)$, and $f_0(600)$ and $f_0(1370)$ as mixtures of the 8th component of octet and the SU(3) singlet. The Gell-Mann–Okubo (GM-O) formula**

$$3m_{f_8}^2 = 4m_{K_0^*}^2 - m_{a_0}^2$$

gives $m_{f_8} = 910$ MeV.

In relation for masses of nonet

$$m_\sigma + m_{f_0(1370)} = 2m_{K_0^*}$$

the left-hand side is by about 18 % bigger than the right-hand one.

- **For the next nonet we find: $a_0(1450)$, $K_0^*(1450)$, and $f_0(1500)$ and $f_0(1710)$, the $f_0(1500)$ being mixed with a glueball which is dominant in this state. From the GM-O formula, $m_{f_8} \approx 1453$ MeV. In formula**

$$m_{f_0(1500)} + m_{f_0(1710)} = 2m_{K_0^*(1450)}$$

the left-hand side is by about 12.5 % bigger than the right-hand one.

This assignment moves a number of questions, stood earlier, and does not put the new ones. The mass formulas indicate to non-simple mixing scheme. The breaking of 2nd relations tells us that the $\sigma - f_0(1370)$ and $f_0(1500) - f_0(1710)$ systems get additional contributions absent in the $K_0^*(900)$ and $K_0^*(1450)$, respectively. A search of the adequate mixing scheme is complicated by the circumstance that here there is also a remainder chiral symmetry, though, on the other hand, this permits one to predict correctly, *e.g.*, the σ-meson mass.